# Modelling of Backward Erosion Piping in Two- and Three- Dimensional Domains

**Chapter** · September 2019

DOI: 10.1007/978-3-319-99423-9_14



2 authors:

Bryant Andrew Robbins
Institute for Water Resources - U.S. Army Corps of Engineers


D. V. Griffiths
Colorado School of Mines

# Modelling of Backward Erosion Piping in Two- and Three- Dimensional Domains

Bryant A. Robbins[1(✉)] and D. V. Griffiths[2]

[1] U.S. Army Engineer Research and Development Centre, Vicksburg, MS, USA
bryant.a.robbins@usace.army.mil
[2] Colorado School of Mines, Golden, CO, USA

**Abstract.** Backward erosion piping is a highly three-dimensional process responsible for the failure of many embankment dams and levees. Unfortunately, the majority of numerical models developed for predicting piping are two-dimensional. This study presents finite element models for backward erosion piping computations in both two- and three-dimensional domains. Analyses results indicate that the degree of concentration of flow in three-dimensional models is much more severe than in two dimensions, resulting in higher estimates of the hydraulic gradient near the upstream end of the erosion channel.

**Keywords:** Backward erosion piping · Finite element model · Dams Levees

## 1 Introduction

Backward erosion piping (BEP) is an internal erosion mechanism by which foundation soil is gradually removed from beneath a water retaining structure such as a dam or levee as shown in Fig. 1. Erosion typically initiates near the downstream embankment toe due to the vertical hydraulic gradient being highest at this location and progresses in the upstream direction along the interface between the sand and a cohesive cover layer. As the erosion channel progresses, groundwater concentrates towards the pipe resulting in a highly three-dimensional flow pattern. Unfortunately, the majority of models developed for predicting BEP are two-dimensional. This paper presents results from both two- and three-dimensional finite element models to examine the impact of this restriction on modelling of erosion progression.

## 2 Previous Studies

Previous research on BEP (de Wit et al. 1981; Hanses 1985; Townsend and Shiau 1986; Schmertmann 2000; van Beek 2015) has provided a general understanding of the physics of the process. Referring to Fig. 1, the process includes (1) Darcian flow; (2) exit related hydraulic conditions, such as orifice flow, pipe flow, or constant head boundary conditions; (3) liquefaction or fluidization at the pipe head due to concentrated flow leading to (4) occasional bursts of high suspension solids into the pipe; (5) laminar flow conditions in the open pipe that cause (6) sediment transport along the


S. Bonelli et al. (Eds.): EWG-IE 2018, LNCE 17, pp. 149–158, 2019.
https://doi.org/10.1007/978-3-319-99423-9_14

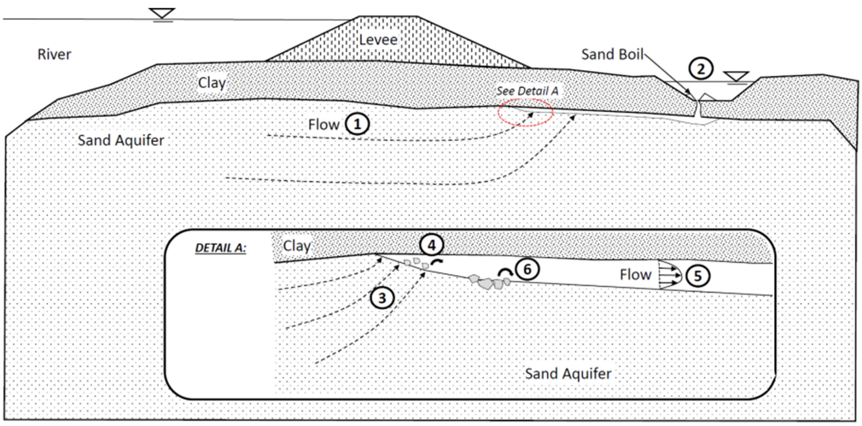


**Fig. 1.** Illustration of the physics of backwards erosion piping.

bottom of the pipe. The concentrated flow at the pipe tip has been shown to control pipe progression (van Beek 2015; Robbins et al. 2018). As the head loss in the pipe influences the hydraulic gradients near the pipe tip, the pipe hydraulics must be accurately accounted for. As such, models for BEP must include features to accurately and independently describe the erosion at the pipe tip, the hydraulic resistance in the pipe, and the groundwater flow.

Numerous investigators have numerically modelled BEP. Wang et al. (2014) classified these models into three broad categories in terms of how the piping process is represented, i.e., (1) models that simply increase pipe zone permeability within a routine seepage analysis (e.g., Vandenboer et al. 2013; Van Esch et al. 2013), (2) multi-phase soil models in which the erosion and transport of eroded particles are explicitly accounted for (e.g., Wang et al. 2014; Fujisawa et al. 2010; Rotunno et al. 2017), and (3) Discrete Element Method (DEM) simulations, typically coupled to a continuum description of fluid flow (e.g., Lominé et al. 2013; Zou et al. 2013; Tran et al. 2017). For analysis of BEP, it is desired to predict ultimate pipe progression limits at the structural scale (i.e. how far will the pipe progress through the foundation?). This question can be conservatively answered using Category 1 models. Given that Category 1 models are also the simplest of the three model categories, this approach was selected for investigating BEP in both two and three dimensions in the following sections.

## 3 Model Descriptions

Custom finite element models for simulating BEP were developed by adapting the steady state groundwater program documented in Smith and Griffiths (2004). Two dimensional models were developed for conducting BEP analysis in both plan view and elevation view (i.e., profile or cross-sectional view). Additionally, a three-dimensional program was developed. The following sections describe the model formulations, first for elevation analysis followed by brief descriptions of the various modifications required for plan view and three-dimensional analysis.

### 3.1 Two-Dimensional Model: Elevation View Analysis

Consider the elevation view of a simple BEP model shown in Fig. 2. The entire domain is constructed of quadrilateral elements, with the pipe domain ($\Omega_p$) being represented by a single row of quadrilateral "pipe" elements and the soil domain ($\Omega_s$) consisting of remaining elements. The flow in the soil ($\Omega_s$) is governed by the Laplace equation which can be solved by finite elements as an equivalent matrix problem given by (e.g., Smith and Griffiths 2004)

$$[K_e]\{H\} = \{Q\} \tag{1}$$

where $\{H\}$ and $\{Q\}$ are vectors of the total head and net flow at the FEM nodes, and $[K_e]$ is the assembly of element conductivity matrices given by

$$[k_e] = \int k_x \frac{\partial N_i}{\partial x}\frac{\partial N_j}{\partial x} + k_y \frac{\partial N_i}{\partial y}\frac{\partial N_j}{\partial y}\, d\Omega_s \tag{2}$$

with $k_x$ and $k_y$ denoting the hydraulic conductivity in the coordinate directions and $N_i$ denoting the finite element shape functions. The flow in the eroded pipe is assumed to be similar to that of 1D laminar flow passing through two parallel plates. This assumption is deemed suitable due to (1) the shallow depth and large width of the erosion channels (Muller-Kirchenbauer et al. 1993) and (2) the laminar flow conditions observed in BEP pipes at the laboratory scale (Robbins et al. 2018). Restricting the model for now to only horizontal pipe progression, the flow through the pipe is related to the hydraulic gradient by

$$q_p = -\frac{a^3 \rho g}{12\mu}\frac{dH}{dx} \tag{3}$$

(Sellmeijer 1988) where $a$ denotes the depth of the eroded pipe, $g$ is the acceleration of gravity, and $\mu$ and $\rho$ represent the dynamic viscosity and density of water, respectively. From continuity,

$$\frac{dq_p}{dx} + S = 0 \tag{4}$$

where $S$ is a sink/source term due to flow along the pipe. Substitution of Eq. 3 into Eq. 4 yields the differential equation governing the pipe flow in $\Omega_p$.

$$\frac{a^3 \rho g}{12\mu}\frac{d^2 H}{dx^2} = S \tag{5}$$

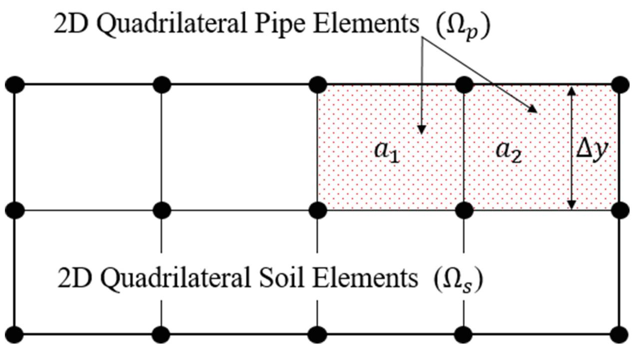


**Fig. 2.** Finite element discretization of BEP

Robbins and Griffiths (2018) demonstrated that Eq. 5 is satisfied in the quadrilateral pipe elements ($\Omega_p$) by assembling the pipe elements into Eq. 1 using Eq. 2 with an equivalent hydraulic conductivity ($k_{pipe}$) substituted for $k_x$ and $k_y$ where

$$k_{pipe} = \frac{a^3 \rho g}{12 \mu \Delta y} \tag{6}$$

with $\Delta y$ denoting the height of the pipe element as shown in Fig. 2 and $a$ denoting the depth of the erosion pipe within each element. This approximation was demonstrated to provide an adequate solution provided the element size used was sufficiently small (0.25 m elements gave essentially the same solution as representing the pipe using 1D rod elements). For complete details, see Robbins and Griffiths (2018).

In addition to satisfying the pipe hydraulics given by Eq. 5, the sand grains in the bottom of the erosion pipe must be in equilibrium. If equilibrium conditions do not prevail, the pipe would deepen further resulting in a different hydraulic solution. The hydraulic shear stress at the bottom of the pipe is determined from force equilibrium to be

$$\tau = \frac{a \rho g}{2} \frac{dH}{dx} \tag{7}$$

The equilibrium condition that must be satisfied is simply given by $\tau < \tau_c$ where $\tau_c$ denotes the critical shear stress for incipient motion of the soil being eroded. The critical shear stress for cohesionless soils can readily be determined from the Shields diagram (Yalin and Karahan 1979). As the pipe depths required for equilibrium are unknown, Picard iterations over the pipe depth, $a$, are conducted to arrive at a satisfactory hydraulic solution satisfying grain equilibrium, pipe hydraulics, and the groundwater flow for a given erosion pipe location. In this study, the pipe depth was incremented by one half of the mean grain diameter ($d$) of the sand each iteration.

Once a hydraulic solution is obtained for a fixed pipe location, the potential for progression of the erosion pipe must be assessed. The pipe progresses further if

$$\frac{\partial H}{\partial x} > i_{crit} \tag{8}$$

in the element immediately upstream of the pipe where $i_{crit}$ is the critical horizontal gradient of the soil being eroded. If Eq. 8 is satisfied in the element immediately upstream of the pipe, the element is switched to a pipe element, and the hydraulic solution must be iteratively solved once again with the new pipe geometry. This process is repeated to evaluate the potential for a pipe to progress through the domain of interest.

### 3.2 Two-Dimensional Model: Plan View Analysis

A plan view analysis only considers the hydraulics of the foundation sand layer. For simplicity, the model assumes a completely horizontal plane, and the pipe can readily progress in any direction in the plane, depending solely on the gradient field for a given problem. Further, it is assumed that no flow passes beneath the pipe elements (all flow in the pipe domain is in the pipe itself). With these assumptions, the equivalent hydraulic conductivity of the pipe ($k_{pipe}$) for plan view analyses is determined to be (following Robbins and Griffiths 2018)

$$k_{pipe} = \frac{a^3 \rho g}{12\mu} \tag{9}$$

Additionally, as the $x$-$y$ plane is now in the horizontal plane, the $x$-$y$ gradient must be used to assess pipe progression resulting in a progression criterion of

$$|\nabla H(x, y)| = \sqrt{\frac{\partial H^2}{\partial x} + \frac{\partial H^2}{\partial y}} > i_{crit} \tag{10}$$

for elements immediately upstream of the pipe. Except for these two changes, the plan view model is identical to the cross-sectional model.

### 3.3 Three-Dimensional Model

In the three-dimensional model, the element height is in the $z$-direction, and the pipe progression was restricted to the $x$-$y$ plane for simplicity. As such, the equivalent hydraulic conductivity for the pipe elements is now given by

$$k_{pipe} = \frac{a^3 \rho g}{12\mu \Delta z} \tag{11}$$

where $\Delta z$ designates the height of the element in the $z$-direction, and the pipe width is determined by the element width. The criterion for pipe progression is once again given by Eq. 10 as the pipe is allowed to progress horizontally in the $x$-$y$ plane.

## 4 Analyses Results

The simple test case illustrated in Fig. 3 was used to perform an initial model comparison. The problem consists of a 10-m soil cube with constant head upstream and downstream boundary conditions. All other boundaries are no-flow boundaries. The pipe is initiated at the top-centre location on the downstream face by changing a single element to a pipe element. An element size of 0.25 m was used in the analysis. Illustrations of the corresponding finite element meshes are shown in Fig. 4 with the pipe progressed 6 m into the domain. All material properties used for the analyses are provided in Table 1. The value of $i_{crit}$ was arbitrarily set to 0.1 (a value less than the average gradient of 0.2) to ensure that the pipe would progress completely through the domain. This was done as the focus of the investigation was on comparing the differences in the hydraulic solutions obtained from the three model formulations.

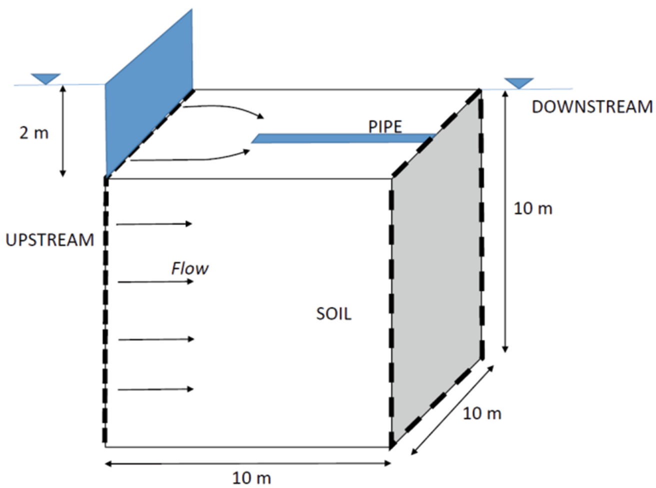


**Fig. 3.** Simple test problem for model comparison.

The pipe was allowed to progress through the domain entirely. For each progression step, the head profile, nodal hydraulic gradients, and calculated pipe depth profile were examined. The step at which the pipe had progressed 6 m through the domain was chosen for comparison purposes as the pipe was sufficiently developed to see differences in the pipe hydraulic computations, but enough soil remained upstream to be able to examine upstream flow patterns. The flow nets for the 2D analyses are illustrated in Fig. 5. The head profiles and pipe depth profiles along the centreline of the pipe are illustrated in Fig. 6. It is readily observed that the head profiles in the pipe are quite similar for all three models. However, the head profile upstream of the pipe is much more non-linear in the three-dimensional model. This is due to the flow concentration that is able to be captured in three dimensions, which results in higher hydraulic gradients.

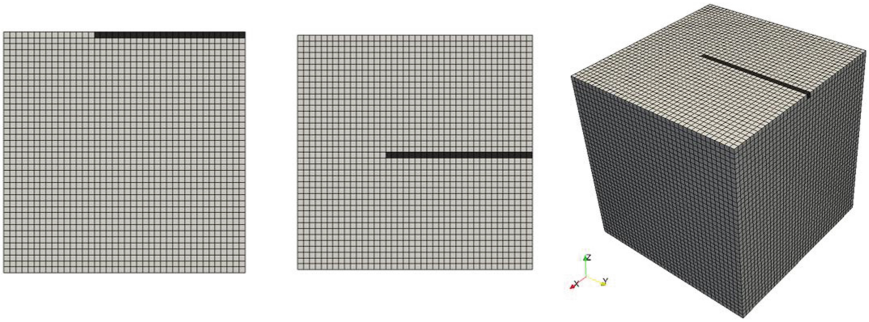

**Fig. 4.** Meshes with pipe progressed 6 m shown for cross-sectional analyses, plan view analyses, and three dimensional analyses (from left to right).

**Table 1.** Material properties and boundary condition for BEP analyses.

| $d$ (mm) | $k$ (m/s) | $\tau_c$ (Pa) | $\mu$ (Ns/m$^2$) | $i_{crit}$ | $\Delta H$ (m) |
|---|---|---|---|---|---|
| 0.2 | $1 \times 10^{-5}$ | 0.33 | $1 \times 10^{-3}$ | 0.10 | 2 |

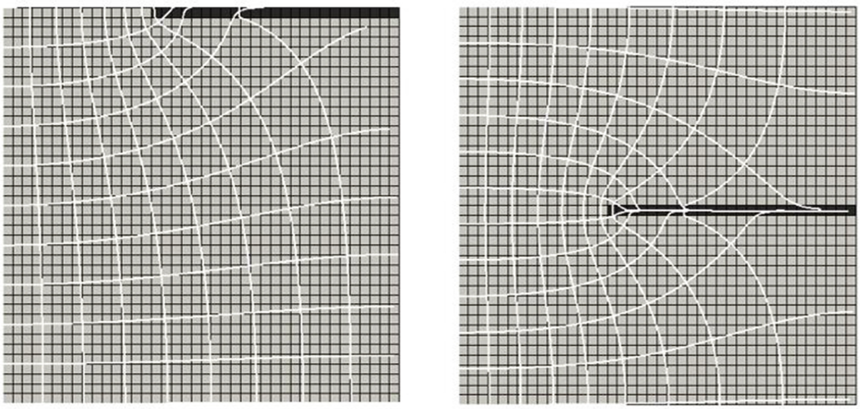

**Fig. 5.** Flow nets with pipe progressed 6 m for cross-sectional analyses and plan view analyses.

As the criterion for pipe progression is the horizontal gradient, a closer examination of the difference in hydraulic gradients upstream of the pipe was needed to fully understand the impacts of the model differences on analyses of pipe progression. To quantify this difference, a concentration factor was defined as

$$F_C = i_{h-3D}/i_{h-2D} \tag{12}$$

with $i_{h-3D}$ and $i_{h-2D}$ designating the horizontal gradient in the element immediately upstream of the pipe from the three-dimensional analyses and two dimensional analysis, respectively. A concentration factor was computed for both the cross-sectional

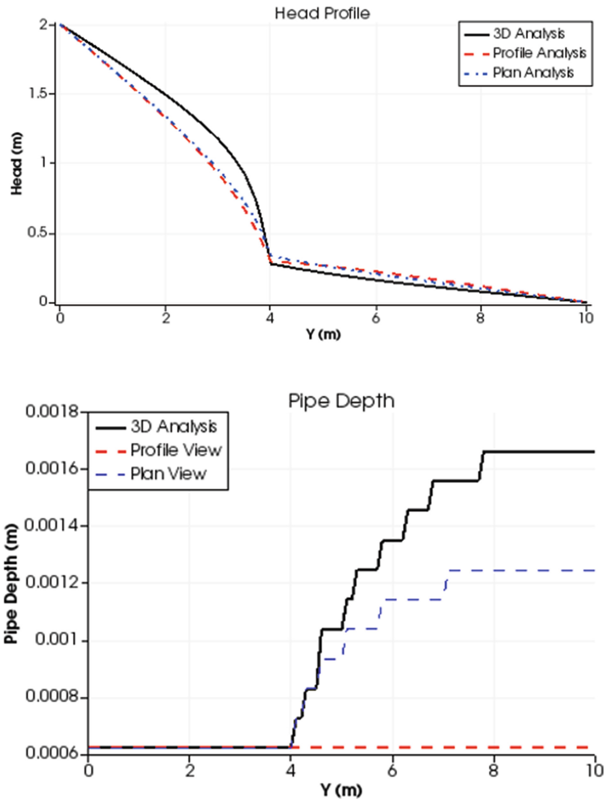


**Fig. 6.** Head profile and pipe depth profile for all three models with the pipe progressed 6 m.

analyses and the plan view analysis. The results are shown in Fig. 7. When the pipe location is furthest downstream, the value of $F_C$ is 1.0 due to no flow concentration occurring into the pipe. As the pipe progresses upstream, the value of $F_C$ increases due to the increasing amount of flow concentration. This indicates that the two-dimensional analyses are not able to fully capture the degree of concentration observed in the 3D model. This is also readily seen in Fig. 6.

## 5 Discussion

This study compared the results of two- and three-dimensional finite element models for piping. While the results indicate that 2D models are not able to fully capture the magnitude of hydraulic gradients upstream of the pipe, this study has been very limited in scope, and further research must be conducted into the relative merits of all three models before firm conclusions may be drawn about the utility of each model. In particular, the following points should be carefully considered.

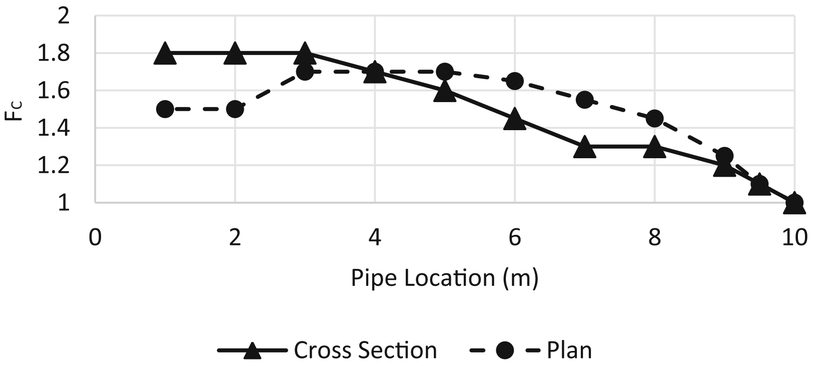


**Fig. 7.** Gradient concentration factors as a function of pipe location.

- The value of $F_C$ increased as the pipe progressed. This may have in part been due to the constant head boundary conditions and small model domain.
- The $F_C$ values presented should not be used until further research into the concentration factors is conducted for full scale levees at critical piping conditions. After further investigation, $F_C$ values may be able to be used to correct 2D models to the equivalent 3D situation.
- Two-dimensional models calibrated to three-dimensional data may inherently include all necessary adjustments.
- The current models do not include widening of the pipe. This may also impact the concentration factors as it will allow more flow to pass through the pipe at the same gradient in both 3D and plan view analysis.
- Underprediction of the upstream gradient as observed in the 2D models may unconservatively predict BEP equilibrium.

Future research must be conducted to better understand the behaviour of the models over a broad range of conditions. Additionally, model validation is required through hindcasting of both experiments and case histories.

## 6 Conclusions

Finite element models for analyses of backward erosion piping were developed in both two and three dimensions. Two-dimensional modelling capabilities were developed for cross sectional analyses and plan view analyses. A simple comparison of the three types of models indicates that the hydraulic gradients upstream of the erosion pipe are much higher in the three-dimensional model than the two-dimensional models. A concentration factor was defined for correcting two-dimensional models. While the direction of this research holds much promise for better understanding of BEP, more research is required before these concepts can be applied in practice.

## References

De Wit JM, Sellmeijer JB, Penning A (1981) Laboratory testing on piping. In: Soil mechanics and foundation engineering, pp 517–520. Rotterdam

Fujisawa K, Murakami A, Nishimura S-I (2010) Numerical analysis of the erosion and the transport of fine particles within soils leading to the piping phenomenon. Soils Found 50 (4):471–482

Hanses U (1985) Zur Mechanik der Entwicklung von Erosionskanälen in geschichtetem Untergrund unter Stauanlagen. Dissertation, Grundbauinstitut der Technischen Universität Berlin, Berlin, Germany (in German)

Lominé F, Scholtès L, Sibille L, Poullain P (2013) Modeling of fluid solid interaction in granular media with coupled lattice boltzmann/discrete element methods: application to piping erosion. Int J Numer Anal Methods Geomech 37(December 2011):577–596. https://doi.org/10.1002/nag

Muller-Kirchenbauer H, Rankl M, Schlotzer C (1993) Mechanism for regressive erosion beneath dams and barrages. In: Brauns H, Schuler R (eds) Filters in geotechnical and hydraulic engineering, The Netherlands

Robbins BA, Griffiths DV (2018) A simplified finite element implementation of the Sellmeijer model for backward erosion piping. In: Proceedings of the 9th European conference on numerical methods in geotechnical engineering. Puerto, Portugal, June 25–27, 2018

Robbins BA, van Beek VM, Lopez-Soto JF, Montalvo-Bartolomei AM, Murphy J (2018) A novel laboratory test for backward erosion piping. Int J Phys Model Geotech 1–14

Rotunno AF, Callari C, Froiio F (2017) Computational modeling of backward erosion piping. In: Models, simulation, and experimental issues in structural mechanics. Springer, Berlin, pp 225–234

Schmertmann JH (2000) The no-filter factor of safety against piping through sands. In: Silva F, Kavazanijian E Jr. (eds) Judgement and innovation pp 65–133. American Society of Civil Engineers

Sellmeijer JB (1988) On the mechanism of piping under impervious structures. Dissertation. Delft University of Technology

Smith IM, Griffiths DV (2004) Programming the finite element method, 4th edn. Wiley, Hoboken

Townsend FC, Shiau J-M (1986) Analytical and experimental evaluation of piping and filter design for sands. Gainesville, Florida

Tran D, Prime N, Froiio F, Callari C, Vincens E (2017) Numerical modelling of backward front propagation in piping erosion by DEM-LBM coupling. Eur J Environ Civil Eng 21(7-8):1–28

van Beek VM (2015) Backward erosion piping: initiation and progression. Dissertation. Delft University of Technology

Vandenboer K, van Beek V, Bezuijen A (2013) 3D FEM simulation of groundwater flow during backward erosion piping. In: Fifth international young geotechnical engineering conference, pp 5–8

Van Esch JM, Sellmeijer JB, Stolle D (2013) Modeling transient groundwater flow and piping under dikes and dams. In: 3rd international symposium on computational geomechanics (ComGeo III), p 9

Wang D-Y, Fu X-D, Jie Y-X, Dong W-J, Hu D (2014) Simulation of pipe progression in a levee foundation with coupled seepage and pipe flow domains. Soils Found 54(5):974–984

Yalin MS, Karahan E (1979) Inception of sediment transport. J Hydraul Div 105(11):1433–1443

Zou Y-H, Chen Q, Chen X-Q, Cui P (2013) Discrete numerical modeling of particle transport in granular filters. Comput Geotech 47:48–56. https://doi.org/10.1016/j.compgeo.2012.06.002